*Baltic Astronomy, vol. xx, xxx–xxx, 2008.*

# CHEMICAL EVOLUTION OF THE GALACTIC BULGE: SINGLE AND DOUBLE INFALL MODELS

R. D. D. Costa W. J. Maciel and A. V. Escudero

*University of São Paulo, Rua do Matão 1226, Cidade Universitária, 04005-000 São Paulo SP, Brazil*

Received 2008; revised 2008

arXiv:0901.4382v1 [astro-ph.GA] 28 Jan 2009

**Abstract.** Recent work has produced a wealth of data concerning the chemical evolution of the galactic bulge, both for stars and nebulae. Present theoretical models generally adopt a limited range of such constraints, frequently using a single chemical element (usually iron), which is not enough to describe it unambiguously. In this work, we take into account constraints involving as many chemical elements as possible, basically obtained from bulge nebulae and stars. Our main goal is to show that different scenarios can describe, at least partially, the abundance distribution and several distance-independent correlationss for these objects. Three classes of models were developed. The first is a one-zone, single-infall model, the second is a one-zone, double-infall model and the third is a multizone, double infall model. We show that a one-zone model with a single infall episode is able to reproduce some of the observational data, but the best results are achieved using a multizone, double infall model.

**Key words:** The Galaxy: chemical evolution – the galactic bulge – planetary nebulae

## 1. INTRODUCTION

The galactic bulge has been extensively studied in the last few years, but many of its properties and formation history are still open to discussion. Among the main bulge characteristics that can be taken as constraints for chemical evolution models are the metallicity distribution, the $\alpha$-element relation to the metallicity, and several abundance correlations that are distance-independent. Concerning stellar data, such constraints have had a considerable improvement in the last couple of years (see for example Rich and Origlia 2005, Cunha and Smith 2006, Fulbright et al. 2006, 2007, Rich et al. 2007, Zoccali et al. 2006, and Lecureur et al. 2007). On the other hand, nebular data have also improved, as can be seen from our own results (Cuisinier et al. 2000, Escudero and Costa 2001, Escudero et al. 2004, Cavichia et al. 2008). Although the chemical abundances of planetary nebulae (PNe) can be obtained with a high accuracy for several elements that are more difficult to study in stars, these results are often overlooked in the literature, despite their importance as constraints for chemical evolution models of the bulge.

Regarding the bulge formation and evolution, a mixed scenario seems to be more attractive. Since the earlier models for bulge stars that could predict ratios of $\alpha$-elements for bulge metallicities (Matteucci and Brocato 1990), several

models adopting a single fast collapse have been proposed. These models are able to explain isolated stellar abundances, but the abundance correlations for large groups of chemical elements are generally not well reproduced. Besides, kinematic evidences point to a bulge rotation profile similar to a disk, but including an additional component with a larger velocity dispersion (Beaulieu et al. 2000). Some recent models have at least partially corrected this situation, as in the theoretical models by Ballero et al. (2006, 2007a,b). In Ballero et al. (2007b), to which the reader is referred for a detailed discussion on previous chemical evolution models for the galactic bulge, observational constraints such as the metallicity distribution and $\alpha$-element ratios as a function of metallicity are well reproduced, especially for oxygen, for which a large variety of observational data is available. The authors claim that there is no need to invoke a second infall episode, but it should be noted that the abundance correlations taken as constraints are limited. In fact, it has become increasingly more difficult to explain all these observations in a satisfactory way using a single infall episode.

In this work we present single- and double-infall models for the bulge evolution, using both planetary nebulae and stellar data as constraints. The PNe data comes basically from our own group, while for stars we have used recent data from the literature. In order to describe the galactic bulge in a less ambiguous way, we made an effort to include as many chemical elements as possible. Our main goal is to show that different scenarios can describe, at least partially, the abundance distribution and other abundance correlations for bulge objects. We show that a one-zone model with a single infall episode is able to reproduce some of the abundance distributions, but the best results are achieved using a multizone, double infall model.

## 2. THE CHEMICAL EVOLUTION MODEL

### *2.1. The Star Formation Rate*

The star formation rate (SFR) is a key factor to describe the chemical evolution of a galaxy, as it gives the total amount of gas converted into stars, which depends on many environmental factors, such as density, temperature, presence of winds, tidal forces, etc. The SFR affects directly nearly all the results of a chemical evolution model, since it modifies not only the amount of stars, but also the gas density of the medium. Most approximations for the SFR are power laws of the gas density, and the usual form is given by the generic Schmidt law:

$$SFR = c\ \sigma^k, \tag{1}$$

where $c$ is a constant, $\sigma$ is the gas density and $k$ a constant greater than unity. The values of the constants $c$ and $k$ are usually derived empirically from observations of spirals and starburst galaxies (Schmidt 1959, Buat et al. 1989, Kennicutt 1998a,b). We have adopted the values derived by Kennicutt (1998b), $c = (2.5 \pm 0.7) \times 10^{-4}$ and $k = 1.4 \pm 0.15$, so that the SFR is given in $M_\odot\,\mathrm{year}^{-1}\,\mathrm{kpc}^{-2}$. In Equation (1), $\sigma$ is then the surface density, which can be related to the average volume density of the gas. These values are generally similar to the values based on SFR derived from $H_\alpha$, UV and FIR data, as given by Buat et al. (1989), Kennicutt (1989), Buat (1992), Boselli (1994), Deharveng et al. (1994), and Boselli et al. (1995).

### *2.2. Infall*

The infall rate is not a well known parameter, and depends on many factors such as the total amount of mass, gas density and gas collisions. We can define the infall rate as an exponential profile of the form $\dot{M}(t) \propto \exp(-t/\tau)$, where $\tau$ is the input timescale to the medium (Chiosi 1980). In spite of being a simplified way to represent the gas increase rate, chemical evolution models have shown good agreement when compared to observational constraints (Chiappini et al. 1997). We can then write

$$\dot{M}(t) = A\ e^{-t/\tau}\ . \tag{2}$$

The proportionality constant can be estimated from the total amount of material, $M_T$:

$$M_T = A\tau\ . \tag{3}$$

To obtain the amount of material falling in a given time interval, the infall rate has to be integrated as:

$$\Delta M = \int_t^{t+\Delta t} \dot{M}(t)dt\ . \tag{4}$$

Therefore, we have an expression for the amount of material accreted by the system for any time interval. However, in an open system such the Galaxy, where the halo mass can be constantly altered due to winds, accretion of satellites or other mechanisms, it is convenient to express this value as a function of the remaining infall mass:

$$M_F = \int_t^{\infty} \dot{M}(t)dt \tag{5}$$

Combining equations (4) and (5) we have:

$$\Delta M(t) = M_F \left(1 - e^{-\frac{\Delta t}{\tau}}\right) \tag{6}$$

### *2.3. Binary Systems and SNIa*

Stars in binary systems can have a different evolutionary path compared to individual stars. Depending on the mass and separation of the components in a pair they can evolve to a Type-Ia supernova when one of the components reaches the Chandrasekhar limit. The way stars combine depends on their mass ratio and lifetime of the components, so that the number of SNIa for each mass interval of the secondary may affect the abundances of the medium. In this work we adopted the formalism by Ferrini et al. (1992, see also Matteucci and Greggio 1986). More recent tratments (cf. Matteucci et al. 2006) based on the assumption that Type-Ia SN originate from CO white dwarfs in binary systems without specifying the degeneracy of the progenitor stars may affect the earlier star formation epochs of the galactic halo, but the main conclusions of this paper for the bulge evolution are probably unchanged.

### *2.4. The IMF and stellar yields*

Stars of different masses have different lifetimes and chemical yields. The IMF is a necessary ingredient of any chemical evolution model, as it gives essentially the total amount of stars in each mass interval, which basically affects the stellar yields. In this work we used the Kroupa (2002) IMF, which provides a more realistic distribution of objects with respect to the observational data. For the initial period of multizone, double infall models, we also used Salpeter's IMF, as explained in Section 4.2. Metallicity dependent yields are still quite uncertain (see for example Matteucci 2001, McWilliam et al. 2008), so that most applications adopt mass-dependent yields. In this work, we have used stellar yields derived from numerical models by van den Hoek & Groenewegen (1997) for intermediate mass stars and Tsujimoto et al. (1995) for Type-II supernovae and SNIa.

### *2.5. Winds*

Galactic winds are important in many chemical evolution models in order to explain the observed abundances in dwarf and elliptical galaxies. However, a detailed and self consistent treatment of the mass loss is too complex, as it depends on factors such as the presence of infall, enviromental gas, external pressures, geometrical distribution, etc. Therefore, the mass loss in the galactic bulge is usually included as a free parameter, as in Ferreras et al. (2003). In this work, we have adopted a similar procedure, and the wind effect was simulated by considering that a fraction of the material ejected by SNII/Ia, considered as a free parameter, is lost to an adjacent region, to the halo or out of the Galaxy.

## 3. THE OBSERVATIONAL SAMPLES

Concerning planetary nebulae, the observations and data reduction procedures are described by Escudero et al. (2004), to which the reader is referred for details. Observations were performed in two telescopes: 1.60 m LNA (Brasópolis - Brasil) and 1.52 ESO (La Silla  Chile) from 2001 to 2003. In both observatories, the observations consisted in long slit spectroscopy using Cassegrain spectrographs, with gratings of 300 l/mm and 600 l/mm respectively, resulting in reciprocal dispersions of 4.4 Å/pixel and 2.2 Å/pixel. Some additional data on PNe taken from the literature are also described in the same paper. The PNe sample is contained within about $\pm 7$ degrees in galactic latitude, to make sure that bulge nebulae only are included. The region within about $\pm 1$ degree is underpopulated in all PNe samples, in view of the large extinction in this region.

Regarding stellar data, several recent sets of observations of bulge stars have also been taken into account. These comprise basically the results of Zoccali et al. (2003, 2006, 2008), Rich and Origlia (2005), Cunha and Smith (2006), Fulbright et al. (2006, 2007), Rich et al. (2007) and Lecureur et al. (2007). For the sake of completeness, the set of bulge-like stars by Pompéia et al. (2003) has also been taken into account. Since these objects may be inner disk stars, a comparison of the results from this sample and the remaining ones may shed some light on the apparently different evolution of the bulge and inner disk.

## 4. MODELS

### *4.1. One-zone models*

Two kinds of one-zone models were elaborated: single and double infall models. Table 1 displays the input parameters adopted for these models. The parameters in columns 2 and 3 are *not* free parameters, and were derived independently of the chemical evolution: M1, the mass of the first infall, corresponds to the mass of the spheroidal component as derived by Amaral et al. (1996); M2, the mass of the second infall, corresponds to the mass of the discoidal component, within the first 1.5 kpc, and was calculated based on the disk radial density profile. Regarding the infall timescales ($\tau_1, \tau_2$) and the wind rate $W$, estimates of the parameter space were made on the basis of model calculations by Mollá et al. (2000). The results for $\tau_1, \tau_2$, and $W$ are shown in columns 4–6 of Table 1, respectively.

**Table 1.** Parameters for the one-zone models.

| Model | M1 ($M_\odot$) | M2 ($M_\odot$) | $\tau 1$ (Gyr) | $\tau 2$ (Gyr) | W |
|---|---|---|---|---|---|
| Single | 1.24E10 | - | 1.0 | - | 40% |
| Double | 1.24E10 | 2.26E9 | 0.1 | 2.0 | 60% |

### *4.2. Multizone double-infall model*

The multizone model is based on a mixed scenario for the bulge evolution. To reproduce the abundance distribution and the correlations between elemental abundances, the adopted model has two main phases: the first one is a fast collapse of the primordial gas, essentially responsible for the bulge formation, and the second is a slower infall of enriched gas that forms the disk. The bulge and central region of the Galaxy were divided into two zones (cf. Table 2), the first one experiencing two gas infall episodes, a 0.1 Gyr collapse and an enriched gas infall lasting 2.0 Gyr, as in the previous models of Table 1. Such a division into two zones was chosen as it reproduces in a more realistic way the galaxy evolution scenario of a first infall forming the central region (zone-0 in the present model) and a second one, of enriched gas, to form the disk. The zones have been divided into concentric rings of radius $R1$, $R2$ at 1.5 kpc intervals, as shown in Table 2. The infall masses are also given in the table, where the second infall mass was derived from the disk density (Rana 1991).

**Table 2.** Parameters of the multizone model.

| zone | R1 (kpc) | R2 (kpc) | M1($M_\odot$) | M2($M_\odot$) |
|---|---|---|---|---|
| 0 | 0.0 | 1.5 | 1.24E10 | 2.26E9 |
| 1 | 1.5 | 3.0 | 0 | 4.75E9 |

To better reproduce the chemical abundances for low mass objects, the bulge evolution was divided into two periods with a different IMF. The duration of each period was selected in order to achieve a best fit when comparing model predictions

to the observational data. Based on hydrodynamical simulations (Samland et al. 1997), we assumed that, at the beginning of the bulge formation, a large amount of the elements produced by SNe can be ejected to the halo and inner disk. Investigations on the variation of the slope of the IMF with respect to physical parameters of the ISM show that it can depend both on the metallicity (Silk 1995) and on temperature and density (Padoan et al. 1997). At the beginning of the bulge formation, the bulge ISM was dense and probably had high velocity dispersion. Adopting this hypothesis, Salpeter's IMF was used in the first 0.6 Gyr, and then Kroupa's IMF for the rest of the evolution. For the first period, we adopted Salpeter's IMF, assuming that 85% of the elements produced by SNe are ejected for the halo and inner disk, 70% of which are ejected out of the bulge and 15% from zone 0 to zone 1. For the subsequent evolution we adopted the Kroupa (2002) IMF with a wind rate of 60%, divided in 45% of which are ejected to outside the bulge and 15% from zone 0 to zone 1. It should be noted that, since zone 1 is formed only by the second gas infall, it does not experience the first period effects.

## 5. RESULTS

### *5.1. Abundance distributions of $\alpha$-elements*

Figure 1 displays the chemical abundance distributions of O, Ar, S and Ne for bulge PNe (histograms) compared to the model predictions. The abcissae show the abundances by number of atoms of each element X, defined as $\epsilon(\mathrm{X}) = \log(\mathrm{X/H})+12$, and the ordinate gives the fraction of objects in the whole sample. In this figure, red lines represent one-zone models: continuous red lines for single infall models and dashed red lines for models with double infall. Black lines represent two-zone models as follows: black continuous lines for the central region (zone 0) and black dashed lines for the outer region (zone 1).

It can be seen that the observed oxygen abundance distribution shows a good agreement with both classes of models. Oxygen abundances in PNe reflect the interstellar abundances at the time the progenitor stars were formed, although a small depletion may be observed due to ON cycling for the more massive progenitors. Results for one-zone and multizone models do not differ strongly, except that zone 1 of the multizone model is more metal rich than zone 0, as expected. A similar effect is apparent for argon and neon. The agreement of the model and observational data in Figure 1 is generally reasonable, considering the simplicity of the models and the fact that the data samples are incomplete. The largest discrepancies between the models and the observed distributions occur for neon, in which case the observed abundance distribution peaks about 0.2 dex higher than predicted. This is typically the expected uncertainty of the data, which can explain the discrepancy, along with the simplicity of the model, as mentioned.

The argon and sulfur data produce a generally better agreement with the models. In the one-zone, one infall model, an infall timescale of 1.0 Gyr was adopted, which makes most of the SNII to be produced in a short time interval. As a consequence, oxygen and neon are also produced in a short time interval, rapidly enriching the ISM. Argon and sulfur, on the other hand, are also produced by SNIa, taking a longer time to be ejected to the ISM with respect to SNII yields.

This effect can be seen in the figure, where the solid red lines show a smaller fraction of enriched material in S and Ar as compared to the dashed red line.

The small differences between model results for the abundance distributions can be an indication that, in the case of PNe, we are observing preferentially objects coming from the first collapse. Most of the objects in the sample are found in relatively high latitudes, which supports this hypothesis.

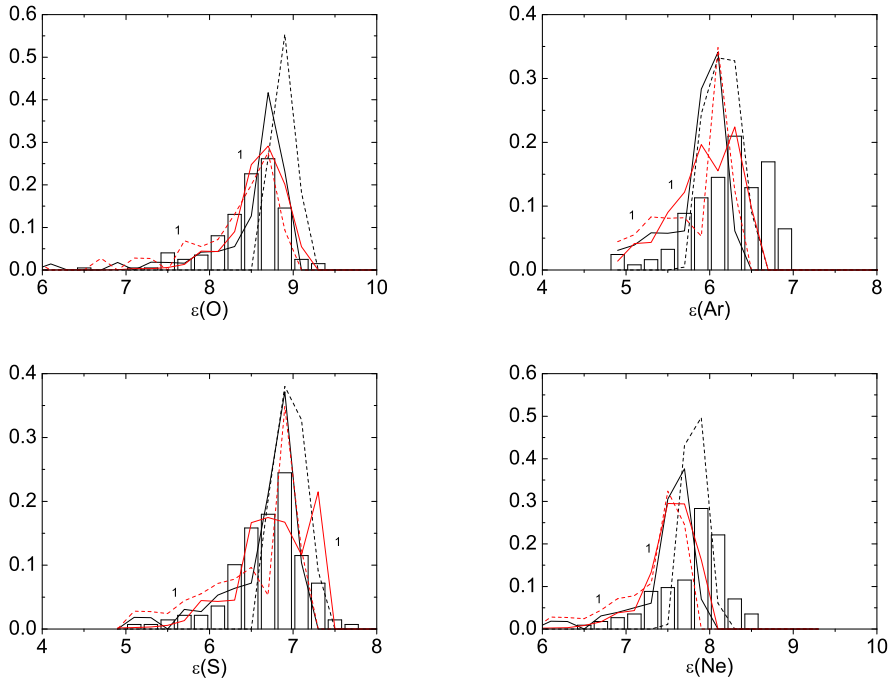


**Fig. 1.** Abundance distribution of $\alpha$-elements derived from PNe (histograms) compared to model predictions. The abcissae show the elemental abundances $\epsilon(\mathrm{X}) = \log \mathrm{X/H} + 12$. Results for one-zone models are shown as red lines: single infall (red continuous lines) and double infall (red dashed lines). For clarity, these models are labelled as "1". Results for multizone models are shown in black: central region (region 0, black continuous lines) and outer region (region 1, black dashed lines).

From Figure 1 we already have an indication that the one-zone models considered in this paper are not able to completely reproduce the observational data. Although a general agreement is achieved, the distributions generally do not match all the observations. In particular, the need of more complex models is apparent from the neon data shown in Figure 1, where the multizone model produces an improved agreement. Such a need is reinforced when one tries to increase the observational constraints by analyzing distance independent abundance correlations, as we will see in the following sections.

*5.2. Metallicity distribution in the bulge*

Another important constraint of chemical evolution models for the bulge is the observed metallicity distribution of bulge stars, as measured by the [Fe/H] ratio. Iron abundances cannot be accurately derived from PNe, since the corresponding lines are very weak and the abundances eventually derived are hampered by the fact that a significant fraction of this element is locked up in grains (cf. Perinotto et al. 1999). Therefore, our predicted metallicity distribution for the bulge, as shown in Figure 2, should be compared with recent determinations of the [Fe/H] metallicity distribution in bulge stars. Such a determination has been provided by Zoccali et al. (2003), based on a combination of near-IR data with optical data. As shown by the histogram of Figure 2, the Zoccali et al. (2003) distribution peaks at near solar value, with a sharp cutoff just above the solar metallicity, and presenting a tail towards lower metallicities down to approximately −1.5 dex. These characteristics are generally well reproduced by our models, particularly in the case of the multizone model.

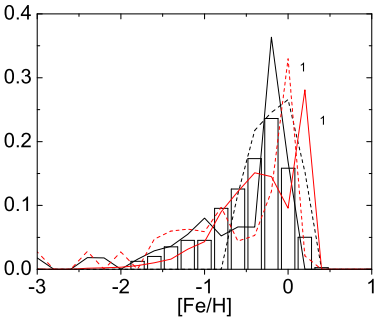


**Fig. 2.** (Left) Metallicity distribution of bulge stars (Zoccali et al. 2003, histogram) and model predictions. Symbols are the same as in Figure 1.

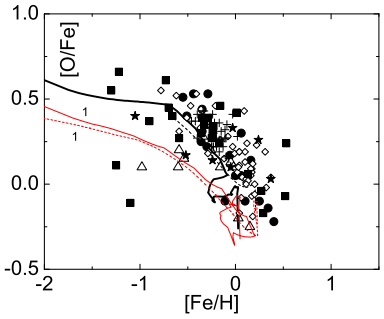


**Fig. 3.** (Right) The [O/Fe] × [Fe/H] relation from our models compared to observational data (see text). Model symbols are the same of Figure 1.

More recently, the bulge metallicity distribution was determined by Rich and Origlia (2005) and Rich et al. (2007) based on infrared spectroscopy of M giants in Baade's Window and in the inner bulge. Although the samples are relatively small, they both agree in the sense that the distribution peaks about [Fe/H] $\simeq -0.2$, in good agreement with the prediction of our multizone model shown in Figure 2. The metallicity distribution of K giants in Baade's Window has also been derived by Fulbright et al. (2006) based on Keck HIRES spectra, with the result that the metallicities range approximately from [Fe/H] $\simeq -1.3$ to $+0.5$, peaking around [Fe/H] $\simeq -0.10$, again near solar value, in agreement with the results previously mentioned. Also, a new recalibration of previous data shows essentially the same characteristics, namely a peak near solar value and a tail towards lower metallicities (see Fulbright et al. 2006 for details). Finally, Zoccali et al. (2008) have presented a detailed metallicity distribution in three fields of the galactic bulge based on 800

K giants using for the first time high resolution spectroscopy of individual stars. The iron distribution function (IDF) for the field $b = -6^{o}$ is roughly similar to the photometric distribution of Zoccali et al. (2003) which is shown in Fig. 2, but extends to slightly larger metallicities, by about 0.2 dex, and presents an excess of objects with metallicities at both sides around -1 dex. As can be seen from Fig. 2, our models have just the same characteristics, extending to slightly higher metallicities than the previous data of Zoccali et al. (2003), and in fact presenting some excess around -1 dex. Therefore, we may conclude that our models, especially the multizone models, show a quite reasonable agreement with recently derived metallicity distributions of bulge stars.

It is interesting to compare the metallicity distribution of Fig. 2 with data from bulge-like stars by Pompéia et al. (2003). The metallicity distribution of these stars is similar to the distribution of true bulge stars, in the sense that it peaks slightly below solar and shows a tail at lower metallicities. This supports the conclusion by Zoccali et al. (2003) and Fulbright et al. (2006) that there is no evidence of any major abundance gradient in the inner bulge, but it should be noted that Zoccali et al. (2008) found some indication of a small gradient in larger fields, and suggested a double-component structure comprising an inner pseudo-bulge within an outer classical bulge.

### *5.3. [α/Fe] correlations with metallicity*

The metallicity dependence of the [O/Fe] ratio of bulge stars is possibly the single most important constraint of chemical evolution models regarding abundance correlations. Figure 3 compares our model predictions for this relation in the galactic bulge with data for bulge stars taken from different sources: Barbuy & Grenon (1990) [triangles], Cunha & Smith (2006) [stars], Fulbright et al. (2007) [squares], Lecureur et al. (2007) [diamonds], Rich & Origlia (2005) and Rich et al. (2007) [crosses]. Model symbols are the same as in Figure 1. These objects are believed to define the behaviour of the [O/Fe] $\times$ [Fe/H] relation in the galactic bulge with a reasonable accuracy, as they include recent, accurate abundance determinations.

It can be seen that the multizone model shows a good fit to the observational data, with a clear improvement relative to the one-zone models. In this case, the difference between our two types of models is much larger than, for instance, in the case of the abundance distribution of PNe data shown in Figure 1. This is a strong indication that a more complex model for the bulge evolution is required. Another feature of our models that is supported by the observations is the relatively low [O/Fe] ratio predicted at low metallicities, in contrast with the models by Ballero et al. (2007b), in which a value of [O/Fe] $\simeq 1$ is obtained. In Figure 3 we also plot the sample of bulge-like stars by Pompéia et al. (2003) [circles]. As in the case of the metallicity distribution (Figure 2), there is no appreciable differences between this sample and the remaining ones, which consist of true bulge stars.

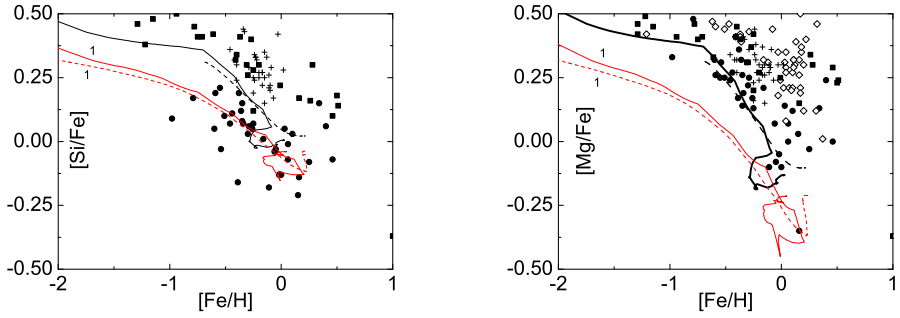


**Fig. 4.** [Si/Fe] and [Mg/Fe] as a function of [Fe/H] for bulge stars. Symbols are as in Figure 3.

Other $\alpha$-elements also show a similar behaviour with metallicity as shown in Figure 4 for the ratios [Si/Fe] and [Mg/Fe]. The symbols are the same as in Figure 3 and the same comments regarding our models apply here. The agreement is reasonable, taking into account that the intrinsic dispersion of the data is much higher. Although these ratios are not as well determined as in the case of oxygen, it is interesting to note that the multizone models show a comparatively better fit to the data than the single zone models.

### *5.4. Abundance correlations in PNe: O, Ne, S, and Ar*

Distance independent correlations of chemical abundances of elements that are not manufactured in the PNe progenitor stars also provide interesting constraints for chemical evolution models, a procedure already successfully used in the galactic disk. Figure 5 shows correlations with oxygen of the Ne, S, and Ar abundances. It can be seen that both classes of models are able to explain reasonably the observed correlations, taking into account the average uncertainties of the abundance determinations, which may reach about 0.2 to 0.3 dex.

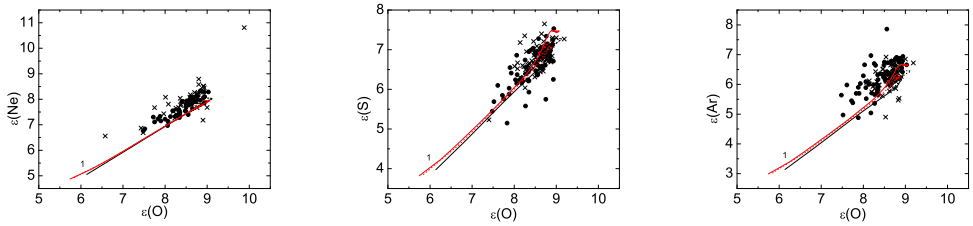


**Fig. 5.** Distance independent correlations of the abundance of Ne, S, and Ar compared to model predictions. Models symbols are as in Figure 1.

### *5.5. Nitrogen abundances*

Nitrogen is an interesting element, in the sense that its abundance can be accurately determined in PNe, in the same way as oxygen. The main difference is

that part of the observed nebular abundances is probably due to the dredge-up episodes occurring in the PNe progenitor stars, which must be taken into account when interpreting N abundances. The N enhancements are modest, and are especially important in the so-called Type I PNe (Peimbert 1978), which comprise a rather small fraction of the observed nebulae. This is recognized for example in the recent models for the bulge by Ballero et al. (2007b), where a sample of bulge PNe was taken into account. Moreover, it has long been known from disk PNe that the N-rich objects have usually $\epsilon(\mathrm{N}) = \log(\mathrm{N/H}) + 12 > 8.0$ (cf. Faúndez-Abans and Maciel 1987), and these objects belong to the high mass end of the intermediate mass stars that originate the PNe, which comprises a relatively small fraction of all PNe progenitor stars. Most of these objects have N-enhancements of a few tenths in the logarithmic scale, while the average N abundance of PNe is about $\epsilon(\mathrm{N}) \simeq 8.0$. Therefore, it is expected that most PNe in the bulge have approximately normal N abundances, a result fully supported by our previous data (Cuisinier et al. 2000, Escudero and Costa 2001, Escudero et al. 2004), so that N could be used – although cautiously – in the comparison with theoretical models, an approach taken by Ballero et al. (2007b).

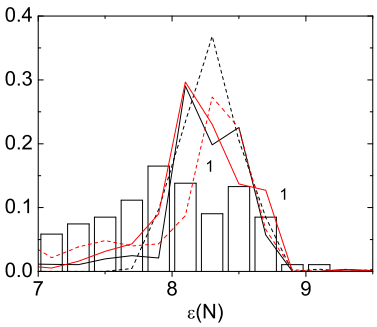


**Fig. 6.** (Left) Abundance distribution of nitrogen compared to model predictions. Symbols are the same as in Figure 1.

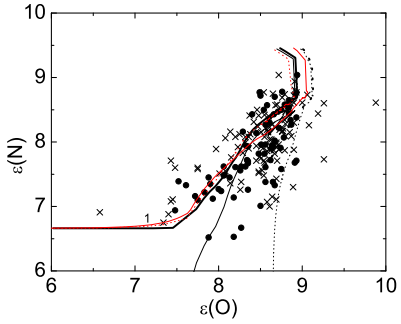


**Fig. 7.** (Right) The same as Figure 5 for nitrogen. Here the multizone model is displayed as black thick lines for the van den Hoek & Groenewegen (1997) yields, black thin lines adopting no yields for N and O for stars with masses smaller than one solar mass and black dotted lines for zone 1.

In Figure 6 we show the observed N abundance distribution along with the theoretical models. Symbols are the same as in Figure 1. We confirm that N abundances peak around $\epsilon(N) \simeq 8$, within the uncertainties, comparable to the disk distribution. The distribution falls abruptly towards higher N abundances, confirming that few objects are strongly N-enhanced and that there is no strong evidence for a recent star formation in the bulge, which would produce many young, massive stars with a high N-enhancement. The nitrogen abundances derived from both models are similar, the multizone models producing a slightly better fit to the data in spite of presenting a narrower distribution with respect to the observational data, and taking into account the probable incompleteness of the observational sample.

In Figure 7 we show the distance-independent correlation of $\epsilon$(N) as a function of $\epsilon$(O) for bulge PNe, which may be compared with Figure 5. Here the black thick lines represent results derived using van den Hoek & Groenewegen (1997) yields and thin black lines represent results derived adopting no yields for nitrogen and oxygen for stars with masses smaller than one solar mass. In these plots the different symbols refer to PNe from different data samples (see Escudero et al. 2004 for details).

From Figure 7 it can be seen that both models are able to reproduce reasonably well most of the data. It can be seen that there is a large scatter in the oxygen abundances for objects with low nitrogen abundances. This scatter can be reproduced assuming that winds produced by SNe of types II and Ia are responsible for the loss of elements synthesized by the SNe, leading to a chemical enrichment of heavier elements such as oxygen and iron relative to lighter elements such as nitrogen and helium. There is also a large number of objects with high oxygen abundances, but with low nitrogen. All one-zone models or those with only primordial gas infall cannot describe this population, which may indicate that these objects originate from an already oxygen-enriched medium. Since it is produced mainly by SNII, this result suggests that this population was formed in an epoch where the gas was already enriched by material ejected by stars with short lifetimes in a medium not yet enriched with elements produced by longer lifetime stars, like nitrogen.

## 6. DISCUSSION

From the results presented in the previous section, there are several evidences in favour of a multizone, double-infall model for the evolution of the galactic bulge, in comparison to a less complex model. In fact, double-infall models have been successfully used to build chemical evolution models for the galactic disk. For example, in the scenario devised by Chiappini et al. (1997), the first infall (with $1.24 \times 10^{10} M_{\odot}$ and 0.1 Gyr timescale) would be responsible for the formation of the old stellar population detected throughout the bulge, and the second episode would represent the gas infall that formed the disk (with $2.26 \times 10^{9} M_{\odot}$ and 2 Gyr timescale), beginning 2 Gyr after the first one. In this model the formation of the bulge is included in the first infall episode forming the halo, and the second infall episode is applied to the disk, while our model assumes two infall episodes to explain the observed properties of the bulge. Any chemical evolution model for the bulge must have a large gas infall episode at the beginning of its formation, in order to reproduce the old population present in that region.

An important observational constraint to the hypothesis of a second infall episode is the presence of an intermediate mass population in the bulge, seen either as PNe or stars (van Loon et al. 2003), since these objects would result directly from the second infall. Observational evidences of a central bar (Bissantz & Gerhard 2002) also favour the hypothesis of a second infall. Therefore, we developed also a double-infall model to better reproduce the observed chemical abundance pattern. In this model we assume that 2% of the mass for the objects between 3 and 16 $M_{\odot}$ generate binary systems that eventually will become SNIa. Yoshii et al. (1996) derived values between 2% and 2.5% when assuming Scalo (1986) IMF and values between 5% and 5.5% adopting Salpeter's IMF. Adopting Kroupa's (2002) IMF, which is very similar to that by Scalo, a value of 2% is

obtained, consistent with disk data.

The galactic bulge had its first star formation episode resulting from a collapse of primordial gas. This episode is a consensus among the recent star formation models. The need of this initial scenario is based not only on results from chemical evolution models but mainly on observational data. Among these is the presence of a large number of old objects, which requires the existence of an extensive star formation at the beginning of the galactic evolution. Also, the wide metallicity distribution found in stars and PNe has to be taken into account. According to the present model, a fast gas collapse is more efficient to form a wide range of metallicities than a slow infall process. A third observational constraint is the presence of old, metal rich stars. An abrupt collapse is able to rapidly enrich the gas, generating both metal-poor and metal-rich stars.

The main characteristics of the first infall is a large mass loss to the outer regions such as the halo, disk or even out of the galaxy, produced by SNII/Ia. This loss of metals is essential to reproduce the observed abundance distributions of PNe. This is also a consensus among the evolutionary models for the bulge. Without this process, stellar abundances would be higher than observed. From our results, the fraction of ejected gas cannot be defined exactly, due to multiple assumptions in the model input. However, it is clear from our results that the multizone model reproduces better the observational constraints. To define this fraction accurately, as well as its time dependence, more accurate observational data and more realistic hydrodynamical models for the central region are required.

The fate of the ejected material is not clear. Samland et al. (1997) suggest that this material was ejected to the halo and eventually fell onto the disk. These authors are able to reproduce different chemical properties of the interstellar medium and the disk. However, one of their conclusions is that the abundance gradient only begun after 6 Gyr, in contradiction to the results from PNe and open clusters (cf. Maciel et al. (2003, 2005, 2006, 2007; Friel et al. 2002), that show the existence of an expressive gradient at that epoch. In the present work, we adopt radial fluxes produced by SN, whose displacement are restricted to the adjacent zone at 1.5 kpc. With this assumption we were able to explain the presence of oxygen-rich and nitrogen-poor planetary nebulae in the bulge.

## 6. CONCLUSIONS

We developed three classes of models to reproduce the abundances of the PNe population of the galactic bulge, representing the chemical evolution of its intermediate mass population, as well as recent data on bulge stars. An effort was made to increase the amount of observational constraints to be explained by the models, so that their reliability is enhanced even though the agreement with the observations might not be perfect. The model results were compared to recent observational data of PNe and stars, leading to the following conclusions: (i) Most of the abundances can be reproduced assuming a fast initial collapse with a high wind rate (ii) Some peculiarities found in the abundances of PNe and bulge stars require the existence of a second infall of material previously enriched by SNII ejecta, and (iii) Abundance ratios from stars ($\alpha$/Fe) suggest that, at the beginning of the bulge formation, the IMF was steeper. The best way to describe it is to assume Salpeter's IMF for the initial 0.6 Gyr and Kroupa's for the rest of the evolution.

ACKNOWLEDGMENTS. This work was partly supported by the Brazilian agencies FAPESP and CPNq. A.V.E acknowledges FAPESP for his graduate fellowship (Proc. 00/12609-0).

REFERENCES

Amaral L. H., Ortiz R., Lépine J. R. D., Maciel W. J. 1996, MNRAS, 281, 339
Ballero S. K., Matteucci F., Chiappini C. 2006, New Astr. 11, 306
Ballero S. K., Kroupa P., Matteucci F. 2007a, A&A 467, 117
Ballero S. K., Matteucci, F., Origlia, L., Rich R. M. 2007b, A&A 467, 123
Barbuy B., Grenon M. 1990, ESO/CTIO Workshop on Bulges of Galaxies, p.83
Beaulieu S. F., Freeman K. C., Kalnajs A. J., Saha P. 2000, AJ 120, 855
Bissantz N., Gerhard O. 2002, MNRAS 330, 591
Boselli A. 1994, A&A 292, 1
Boselli A., Gavazzi G., Lequeux J., Buat V., Casoli F., et al. 1995, A&A 300, L13
Buat V., Deharveng J. M., Donas J. 1989, A&A 223, 42
Buat V. 1992, A&A 264, 444
Cavichia O., Costa R. D. D., Maciel W. J. 2008, (in preparation)
Chiappini C., Matteucci F., Gratton R. 1997, ApJ 477, 765
Chiosi C. 1980, A&A 83, 206
Cuisinier F., Maciel W. J., Köppen J., Acker A., Stenholm B. 2000, A&A 353, 543
Cunha K., Smith V. V. 2006, ApJ 651, 491
Deharveng J. M., Sasseen T. P., Buat V., Bowyer S., Lampton M., Wu X. 1994, A&A 289, 715
Escudero A. V., Costa R. D. D. 2001, A&A 380, 300
Escudero A. V, Costa R. D. D., Maciel W. J. 2004, A&A 414, 211
Faúndez-Abans M., Maciel W. J. 1987, A&A 183, 324
Ferreras I., Wyse R. F. G., Silk J. 2003, MNRAS 345, 1381
Ferrini F., Matteucci F., Pardi C., Penco U. 1992, ApJ 387, 138
Friel E. D., Janes K. A., Tavarez M., Scott J., Katsanis R., Lotz J., Hong L., Miller N. 2002, AJ, 124, 2693
Fulbright J. P., McWilliam A., Rich R. M. 2006, ApJ 636, 821
Fulbright J. P., McWilliam A., Rich R. M. 2007, ApJ 661, 1152
Kennicutt R. C. 1989 ApJ 344, 685
Kennicutt R. C. 1998a, ApJ 498, 541
Kennicutt R. C. 1998b, ARA&A 36, 189
Kroupa P. 2002, Science 295, 82
Lecureur A., Hill V., Zoccali M., Barbuy B., Gómez A., Minniti D., Ortolani S., Renzini A. 2007, A&A 465, 799
Maciel W. J., Costa R. D. D., Uchida M. M. M. 2003, A&A 397, 667

Maciel W. J., Lago L. G., Costa R. D. D. 2005, A&A 433, 127

Maciel W. J., Lago L. G., Costa R. D. D. 2006, A&A 453, 587

Maciel W. J., Quireza C., Costa R. D. D. 2007, A&A 463, L13

Matteucci F. 2001, The Chemical evolution of the Galaxy, Kluwer

Matteucci F., Brocato E. 1990, ApJ 365, 539

Matteucci F., Greggio L. 1986, A&A 154, 279

Matteucci F., Panagia N., Pipino A., Mannucci F., Recchi S., Della Valle M., 2006, MNRAS 372, 265

McWilliam A., Matteucci F., Ballero S., Rich R. M., Fulbright J. P., Cescutti G. 2008, AJ 136, 367

Mollá M., Ferrini F., Gozzi G. 2000, MNRAS 316, 345

Padoan P., Nordlund A. P., Jones B. J. 1997, MNRAS 288, 145

Peimbert M. 1978, IAU Symp. 76, ed. Y. Terzian, Reidel, p. 215

Perinotto M., Bencini C. G., Pasquali A., Manchado A., Rodriguez Espinosa J. M., Stanga R. 1999, A&A 347, 967

Pompéia L., Barbuy B., Grenon M. 2003, ApJ 592, 1173

Rana N. C. 1991, ARA&A 29, 129

Rich R. M., Origlia L. 2005, ApJ 634, 1293

Rich R. M., Origlia L., Valenti E. 2007, ApJ 665, L119

Samland M., Hensler G., Theis Ch. 1997, ApJ 476, 544

Scalo J. M. 1986, Fund. Cosmic Phys. 11, 1

Schmidt M. 1959, ApJ 129, 243

Silk J. 1995, ApJ 438, L41

Tsujimoto T., Nomoto K., Yoshii Y., Hashimoto M., Yanagida S., Thielemann F. K. 1995, MNRAS 277, 945

van den Hoek L. B., Groenewegen M. A. T. 1997, A&AS 123, 305

van Loon J. Th., Gilmore G. F., Omont A. et al. 2003 MNRAS 338, 857

Yoshii Y., Tsujimoto T., Nomoto K. I. 1996, ApJ 462, 266

Zoccali M., Hill, V., Lecureur, A., Barbuy, B., Renzini A., Minniti, D., Gómez, A., Ortolani S. 2008, A&A 486, 177

Zoccali M., Lecureur A., Barbuy B., Hill V., Renzini A., Minniti D., Momany Y., Gómez A., Ortolani S. 2006, A&A 457, L1

Zoccali M., Renzini A., Ortolani S., Greggio L., Saviane I., Cassisi S., Rejkuba M., Barbuy B., Rich R. M., Bica E. 2003, A&A 399, 931